JGV Papers in Press. Published November 25, 2009 as doi:10.1099/vir.0.017327-0

Characterization of a novel wood mouse virus related to murid herpesvirus 4

David J. Hughes[1,], Anja Kipar[2], Steven G. Milligan[3], Charles Cunningham[3], Mandy Sanders[4], Michael A. Quail[4], Marie-Adele Rajandream[4], Stacey Efstathiou[5], Rory J. Bowden[3], Claude Chastel[6], Malcolm Bennett[2], Jeffery T. Sample[7], Bart Barrell[4], Andrew J. Davison[3] and James P. Stewart[1*]

[1] School of Infection and Host Defence, University of Liverpool, Liverpool L69 3GA, UK
[2]Department of Veterinary Pathology, University of Liverpool, Liverpool, L69 7ZJ, UK
[3]MRC Virology Unit, Institute of Virology, University of Glasgow, Church Street, Glasgow G11 5JR, UK
[4]The Wellcome Trust Sanger Institute, The Wellcome Trust Genome Campus, Cambridge, CB10 1SA, UK
[5]Division of Virology, Department of Pathology, University of Cambridge, Tennis Court Road, Cambridge CB2 1QP, UK
[6]Laboratoire de Virologie, Faculté de Médecine, 29285 Brest, France
[7]Department of Microbiology and Immunology, The Pennsylvania State University College of Medicine, Hershey, PA 17033, USA

[*]**Corresponding author:** James P. Stewart, School of Infection and Host Defence, University of Liverpool, Liverpool L69 3GA, UK. Tel: +44 151 706 4381. E-mail: j.p.stewart@liv.ac.uk.

Present address: David J. Hughes, Department of Microbiology and Immunology, The Pennsylvania State University College of Medicine, Hershey, PA 17033, USA

Present address: Steven G. Milligan, Infection and Immunity Section, Level 9, University of Glasgow Dental School, 378 Sauchiehall Street, Glasgow G2 3JZ, UK

Present address: Rory J. Bowden, Oxford Centre for Gene Function, Department of Statistics, 1 South Parks Road, Oxford, OX1 3TG, UK

Words in summary: 206
Words in main text: 5425
Figures and Tables: 8 + 1 Supplementary Table

Contents category: Animal Viruses – Large DNA

Running title: Wood mouse herpesvirus

The DNA sequences of WMHV and BRHV were deposited in GenBank under accession numbers GQ169129 and EF495130, respectively.

SUMMARY

We have isolated two novel gammaherpesviruses, one from a field vole (*Microtus agrestis*) and the other from wood mice (*Apodemus sylvaticus*). The genome of the latter, wood mouse herpesvirus (WMHV), was completely sequenced. WMHV had the same genome structure and predicted gene content as murid herpesvirus 4 (MuHV4; murine gammaherpesvirus 68). Overall nucleotide sequence identity between WMHV and MuHV4 was 85 % and most of the 10 kbp region at the left end of the unique region is particularly highly conserved, especially the viral *tRNA*-like sequences and the coding regions of genes *M1* and *M4*. The partial sequence (71913 bp) of another gammaherpesvirus, Brest herpesvirus (BRHV), which was isolated ostensibly isolated from a white-toothed shrew (*Crocidura russula*), was also determined. The BRHV sequence was 99.2 % identical to the corresponding portion of the WMHV genome. Thus, WMHV and BRHV appear to be strains of a new virus species. Biological characterization of WMHV indicated that it grows with similar kinetics to MuHV4 in cell culture. The pathogenesis of WMHV in wood mice was also extremely similar to that of MuHV4, except for the absence of inducible bronchus-associated lymphoid tissue at day 14 post infection and a higher load of latently infected cells at 21 days post infection.

INTRODUCTION

The most extensively characterized members of the family *Herpesviridae* that have hosts in the family Muridae are mouse cytomegalovirus (MCMV) and rat cytomegalovirus (RCMV), which are classified in the genus *Muromegalovirus* of the subfamily *Betaherpesvirinae*, and murid herpesvirus 4 (MuHV4; also known as murine gammaherpesvirus 68, often abbreviated to MHV-68 or γHV-68; species *Murid herpesvirus 4*), classified in the genus *Rhadinovirus* of the subfamily *Gammaherpesvirinae* (Davison *et al.*, 2009; Efstathiou *et al.*, 1990). Species in the genus *Rhadinovirus* also represent five herpesviruses of primates and one of ungulates. However, these viruses are not closely related to MuHV4, and the best estimate is that the lineages within the genus diverged approximately 60 million years ago (McGeoch *et al.*, 2005). At least three other murid herpesviruses have been reported, though these are unclassified at present (Davison *et al.*, 2009).

MuHV4 was originally isolated from bank voles (*Myodes glareolus*) and yellow-necked field mice (*Apodemus flavicollis*) in Slovakia (Blaskovic *et al.*, 1980); reviewed in (Nash *et al.*, 2001). An epidemiological survey of MuHV4 infection in free-living rodents in the UK (Blasdell *et al.*, 2003) showed that MuHV4 is endemic in wood mice (but not bank voles), indicating that the wood mouse is a major natural host for this virus. Recent definitive molecular data has also shown that MuHV4 is present in free-living yellow-necked field and wood mice (Ehlers *et al.*, 2007).

In consideration of these observations, a wood mouse infection model was developed as an alternative to a model utilizing the laboratory (house) mouse (*Mus musculus*), which has been used to date for MuHV4 studies (Hughes *et al.*, submitted). In comparison with the BALB/c laboratory mouse, the features of MuHV4 infection in the wood mouse are: (i) after intranasal inoculation, viral titres achieved in the lung are approximately 1000-fold lower; (ii) replication is restricted to scattered alveolar epithelial cells and macrophages within focal granulomatous infiltrations, rather than being evident as a diffuse, T-cell dominated

interstitial pneumonitis; (iii) latently infected lymphocytes are abundant in inducible bronchus-associated lymphoid tissue (iBALT); (iv) the spleens of wood mice show reduced splenomegaly and leukocytosis; (v) well-delineated secondary follicles with classical germinal centres are formed; and (vi) titres of neutralizing antibody to MuHV4 are significantly higher.

The present study focuses on the isolation and genetic and biological characterization of a novel, MuHV4-like virus. Two independent strains were examined, one isolated in the present study from wood mice in Cheshire, UK and the other from a white-toothed shrew (*Crocidura russula*) in Brest, France (Chastel *et al.*, 1994).

RESULTS

Genomic characterization of WMHV and BRHV

Three distinct viruses were obtained from free-living murids captured in Cheshire, UK. The isolation and TEM results are summarized in Table 1.

The TEM-positive samples gave rise to PCR products from the DPOL gene, and the TEM-negative samples did not (data not shown). The sequences of the 213-bp amplicons originating from WM1, WM2, WM7 and WM8 DPOL were identical to each other, regardless of the tissue from which the viruses were isolated. These sequences (minus the primers; 160 bp) exhibited 89 % nucleic acid identity and 94 % predicted amino acid sequence identity to the corresponding region of MuHV4 DPOL. The FV1 DPOL amplicon was also 213 bp in size, and the 160-bp sequence (minus primers) was more closely related to MuHV4 than any other herpesvirus, at 61 % nucleic acid and 54 % amino acid sequence identity. The HM4 virus DNA yielded a DPOL PCR product of 231 bp (178 bp minus primers) that was closely related to MCMV (strain Smith) DPOL, at 99 % nucleic acid and 100 % amino acid sequence identity. These results confirm the identification of two novel gammaherpesviruses. The WM isolates were designated WMHV, and the FV1 isolate was designated field vole herpesvirus (FVHV).

An initial analysis of the coding regions of genes *M1*, *M2* and *M3*, which had been identified hitherto only in MuHV4, showed that cognate PCR products were detected in all WMHV isolates using MuHV4-specific primers, thus confirming the close relatedness of these isolates to MuHV4 (Fig. 1). In contrast, none of these genes were amplified from FVHV, consistent with its more distant relationship to MuHV4. The DNA sequences obtained from these PCR products for WMHV *M1* and *M3* were 97 % and 94 % identical to MuHV4 *M1* and *M3*, respectively, while WMHV and MuHV4 *M2* sequences were more divergent, sharing only 83 % identity.

The complete nucleotide sequence of the WMHV genome was then determined. The

genome structure deduced from the WMHV genome sequence is the same as that of MuHV4, consisting of a unique region (U) flanked at both ends by multiple direct repeats of a terminal repeat (TR). In WMHV and MuHV4, the size of U is 118864 and 118211 bp, respectively, and that of TR is 1244 and 1240 bp. Overall nucleotide sequence identity is 85 %. The predicted gene content of WMHV is the same as that for MuHV4, as represented by the most up-to-date annotation (NC_001826). A 71913-bp segment of the BRHV genome was sequenced. This represented TR (1265 bp; plus a partial copy) linked to the left portion of U (70439 bp) terminating within *ORF53*. The BRHV sequence is 86 % and 99.2 % identical to the corresponding portion of the MuHV4 and WMHV genomes, respectively. The information used to annotate the genome sequences is shown in Supplementary Table S1.

Fig. 2 shows a representation of DNA sequence identity along the entire WMHV and MuHV4 genomes, and Fig. 3 provides detail on amino acid sequence identity between WMHV, BRHV and MuHV4 protein-coding regions. The most highly conserved regions between WMHV and MuHV4 include two sets of internal tandem repeats and the region from the left end of U to the end of the *M4* coding region, which includes the eight viral tRNA-like genes (*vtRNAs*) (Bowden *et al.*, 1997). Although the *vtRNAs* are well conserved, there are functionally relevant differences in the sequences of micro-RNAs (*miRNAs*) 1, 2, 5, 6 and 9 that are derived from *vtRNA* primary transcripts (Pfeffer *et al.*, 2004)(Fig. 4). The most highly conserved coding regions at the amino acid sequence level are M4 (98.3 %), ORF43 (97.2 %), M1 (96.9 %) and ORF60 (96.7 %), and the least conserved are ORF73 (67.0 %), ORF51 (68.0%) and M2 (72.8 %). In the comparable sequences, the most highly conserved coding regions at the amino acid sequence level between WMHV and BRHV are ORF8, ORF28, ORF29, ORF34, ORF43, ORF44 and ORF46 (each 100 %), and the least conserved are ORF45 (95.2 %), ORF51 (95.8 %) and M2 (97.4 %). Fig. 5 shows the amino acid sequence alignments for M1, M3 and M4 (which are related), and also M2, ORF51 and ORF73.

Biological characterization of WMHV

The relative rates of growth of MuHV4 and WMHV in NIH3T3 cells were compared by determining a one-step growth curve as described previously (Macrae *et al.*, 2001), and were not significantly different (data not shown).

Fig. 6 shows the features of infection of wood mice by WMHV in comparison with MuHV4. Infectious virus was detected in the lungs of wood mice infected with WMHV or MuHV4 at 7 d PI, but not at 14 d PI, and a significantly greater amount of infectious virus was recovered from MuHV4-infected wood mice at 7 d PI (Fig. 6a). The numbers of leukocytes per spleen isolated from infected wood mice were similar for WMHV and MuHV4 at all time points PI (Fig. 6b). There was an increase in the number of leukocytes at 14 d PI with both viruses, but this was marginal and transient, and infection with neither virus induced significant splenomegaly. In WMHV- and MuHV4-infected wood mice, the number of latently infected cells per spleen increased dramatically from 7 d PI, peaking at 14 d PI (Fig. 6c); the mean number of latently infected cells then declined approximately six-fold by 21 d PI in WMHV-infected animals and twenty-five-fold in the MuHV4-infected mice, and was largely unchanced at 28 d PI in both infections. The difference observed at 21 d PI was statistically significant ($P<0.05$).

Histological examination identified broadly similar changes in both WMHV- and MuHV4-infected wood mice and similar to those reported in detail previously (D.J. Hughes et al. Submitted). On day 7 PI, mild to moderate perivascular or peribronchial, B cell dominated lymphocyte infiltration with evidence of B cell emigration from blood vessels was seen together with multifocal, predominantly perivascular macrophage and lymphocyte (i.e., granulomatous) infiltrates. There was a mild to moderate increase in the number of disseminated T and B cells in the interstitium. Viral antigen was scarce and seen in occasional alveolar epithelial cells (type I and II pneumocytes) and in macrophages within the granulomatous infiltrates. The mediastinal lymph nodes and spleens of these animals

contained primary and secondary follicles and unaltered T cell zones. Rare virus antigen-positive macrophages were seen in the lymph nodes. At 14 d PI, wood mice infected with MuHV4 displayed intense perivascular and peribronchial, B cell rich lymphocyte infiltration with evidence of lymphatic follicle formation (Fig. 7a, b). This has been described previously as being iBALT (D.J. Hughes, submitted). In contrast, in WMHV-infected animals moderate multifocal perivascular and peribronchial B cell infiltration and emigration was seen, but without distinct evidence of follicle formation (Fig. 7c, d). Granulomatous infiltrates were still observed in both groups; these contained macrophages exhibiting viral antigen. Large, well delineated secondary follicles were observed in the spleens, and virus antigen-positive macrophages were detected in the red pulp. At 20 d PI, both granulomatous infiltrates and perivascular and peribronchial lymphocyte infiltrations were still observed in the lungs. However, the follicle formation that was previously seen in MuHV4-infected wood mice had subsided. Spleens exhibited smaller secondary follicles than at day 14 PI. Virus antigen-laden macrophages were seen in the spleen. In the lung, however, viral antigen expression was restricted to one individual macrophage in a granulomatous infiltrate in a MuHV4-infected animal. By day 28 PI, the granulomatous infiltrates were few in number and small, but a mild to moderate perivascular and peribronchial lymphocyte infiltration remained. This persisted until day 46 d PI, to a mild degree. Thus, the changes observed were extremely similar except for the less intense B cell infiltration and absence of iBALT in the lungs of WMHV-infected mice at day 14 PI.

DISCUSSION

This study demonstrated the abundance of herpesviruses in natural populations of wood mice in Cheshire. Two novel gammaherpesviruses (FVHV and WMHV) were isolated. Previous analyses have concluded that herpesvirus genomes of less than 95 % nucleotide sequence identity may represent different species (Ehlers *et al.*, 2007). Thus, the degree of divergence between WMHV and MuHV4, both overall (85 %) and within specific loci (e.g., *M2* and *ORF73*) (Figs. 2, 3), is probably sufficient to warrant classification of WMHV as a new species. Under the current taxonomic scheme, in which murid herpesvirus species are named after the host family, this would be *Murid herpesvirus 7*. Although an epidemiological study of free-living rodents in the UK was unable to distinguish between the two viruses (Blasdell *et al.*, 2003), a PCR-based study of mice trapped in Germany (Ehlers *et al.*, 2007) indicated that MuHV4 is present predominantly in yellow-necked field mice (*Apodemus flavicollis*), whereas WMHV is present in wood mice (*A. sylvaticus*). However, MuHV4 was detected in some wood mice. Thus, it is possible that the two viruses normally infect different *Apodemus* species, but that there is some crossover. The biological characteristics of the two viruses in the wood mouse model exhibit significant similarities. However, the viruses do differ in their ability to grow in the lungs, in the development of iBALT, and also perhaps in the efficiency of reactivation from splenic leukocytes. Interestingly, WMHV was isolated from trigeminal ganglia as well as spleens, suggesting that this virus may be neurotropic during a natural infection. This hypothesis warrants further investigation.

The analysis of the sequence of a large portion of the genome of the BRHV genome showed that the relationship of this virus to WMHV is sufficiently close (99 % identity) to warrant the consideration of WMHV and BRHV as strains of the same virus. Given that herpesviruses are thought generally to have evolved with their hosts (McGeoch *et al.*, 2006), this relationship was unanticipated, since the wood mouse and white-toothed shrew are classified in different mammalian orders, *Rodentia* (family *Muridae*) and *Insectivora* (family *Soricidae*), respectively. Thus, the claimed insectivore source of BRHV must be viewed as

questionable. It is possible that the virus actually originated from a rodent, either by cross-infection in the wild or by laboratory contamination, since BRHV was isolated by passage in suckling mouse brains (Chastel *et al.*, 1994).

Other viruses related to MuHV4 have been characterized, but none thus far has been shown to be sufficiently divergent from MuHV4 to form a new species. Viruses isolated from bank voles or yellow-necked field mice at the same time as MuHV4 (MHV-76, MHV-72, MHV-60 and MHV-78) are considered to be strains of MuHV4. MHV-76, although originally characterized as a novel alphaherpesvirus due to its cytopathic effect *in vitro* (Ciampor *et al.*, 1981; Svobodova *et al.*, 1982) and then as a betaherpesvirus (Hamelin & Lussier, 1992), was conclusively demonstrated to be a gammaherpesvirus (Macrae *et al.*, 2001). MHV-76 proved to be equivalent to MuHV4 with a 9538-bp deletion at the left end of U, which probably arose during passage of the virus *in vivo* or *in vitro*. MHV-72 *ORF21* (encoding thymidine kinase) is identical in sequence to the corresponding MuHV4 gene (Raslova *et al.*, 2000), and *ORF51* (encoding gp150) differs by five nucleotide substitutions (Macakova *et al.*, 2003). Analysis of 12 other loci has shown that MHV-72 is more divergent from MuHV4 than MHV-76, and that *M1*, *M2* and *M3* are absent; nonetheless, MHV-72 and MuHV4 are highly related (Oda *et al.*, 2005). It seems likely that uncharacterized herpesviruses (MHV-60 and MHV-78) isolated at the same time as MuHV4 may also be strains of MuHV4 (Mistríková *et al.*, 2000; Nash *et al.*, 2001).

The WMHV genome is co-linear with that of MuHV4, and the two viruses have the same predicted gene content (Figs. 2, 3). The reason for the generally higher degree of conservation of sequences near the left end of U is not known. Speculative explanations could centre on selective sweeps in this region of the genome or recombination between a WMHV-like virus and a virus more closely related to MuHV4. The noncoding sequences in this region, including the *vtRNA*-like transcripts, are generally highly conserved. However, there are differences in *miRNAs* 1, 2, 5, 6 and 9 that are derived from the primary transcripts

of these *vtRNA*s (Pfeffer *et al.*, 2004) (Fig. 4) . The targets and exact functions of these *miRNAs* are not currently known (Pfeffer *et al.*, 2004), but these differences could have functional consequences and the comparative data could be informative. In addition to noncoding regions in this locus, the M1 and M4 proteins are highly conserved (Fig. 5). It has been proposed that the most likely function for the M4 protein is as a modulator of the innate immune system. *M4* is expressed *in vitro* with kinetics similar to immediate-early genes (Ebrahimi *et al.*, 2003), and *in vivo* it is expressed during productive infection but not during latency (Virgin *et al.*, 1999). M4 does not appear to have a role during the initial stages of infection *in vivo*, but is important during establishment of latency in the spleen (Evans *et al.*, 2006; Geere *et al.*, 2006). M1 has been shown to stimulate a $V\beta4^{+}$ $CD8^{+}$ T cell in a way reminiscent of a superantigen and by doing this facilitate latent infection (Evans *et al.*, 2008).

The M3 protein, which is related to M1 and M4, is also well conserved, but somewhat less so than the M1 and M4 proteins, particularly towards the N terminus (Fig. 2). The secreted M3 protein is expressed strongly during lytic infection and probably to a lesser extent during latency (Simas *et al.*, 1999; Usherwood *et al.*, 2000; van Berkel *et al.*, 1999; Virgin *et al.*, 1999). *In vitro,* the M3 protein selectively binds chemokines associated with the antiviral inflammatory response (Parry *et al.*, 2000; van Berkel *et al.*, 2000). In the laboratory mouse, M3 was found to have a role in enhancing the amplification of latently-infected B cells by affecting the CD8+ T cell response (Bridgeman *et al.*, 2001), although this function was not seen in an independent study (van Berkel *et al.*, 2002). In the wood mouse model, M3 has a critical role in the amplification of latently-infected B cells in the lung and the formation of iBALT containing these cells (Hughes et al, submitted for publication). Differences in M3 may therefore account for the lack of iBALT in WMHV-infected wood mice.

The M2 protein is the most divergent of the four proteins encoded by the left end of the genome, and is associated with latency (Husain *et al.*, 1999). Numerous reports largely agree that *M2* is dispensable for long-term persistence, although MuHV4 recombinants

248 lacking a functional *M2* gene are less efficient in the establishment of latency following
249 intranasal infection of mice (Clambey *et al.*, 2002; Jacoby *et al.*, 2002; Macrae *et al.*, 2003;
250 Simas *et al.*, 2004). It has also been postulated that *M2* is required for efficient colonization
251 of follicle B cells and the development of these cells into memory B cells, a cell type
252 exploited by MuHV4 for long-term latency (Simas *et al.*, 2004). Given the relationship, and
253 possible overlap, between the hosts of WMHV and MuHV4, the divergence of the *M2* gene
254 in a region of low overall variation might reflect strong immune selection. Indeed, it has been
255 shown that an H2-Kd–restricted CD8+ T cell epitope present in M2 (Husain *et al.*, 1999) sets
256 the latent load during persistent infection of laboratory mice (*M. musculus*) (Marques *et al.*,
257 2008). However, this epitope is not conserved between MuHV4 and WMHV (Fig. 5b),
258 suggesting that it may not be functional in the *Apodemus* hosts. The generation of greater
259 numbers of infective centres (a measure of latency) in the spleens of the WMHV-infected
260 wood mice at 21 d PI (Fig. 6c) raises the possibility that M2 may have evolved in this virus to
261 augment the expansion of latently infected cells during the acute phase of latency.
262 Experiments to address this hypothesis could involve replacing MuHV4 *M2* with WMHV *M2*
263 and testing the phenotype in wood mice. Furthermore, numerous PXXP motifs are found
264 throughout MuHV4 M2 (labelled P1-9, Fig.6c), some of which have been shown to
265 functionally bind SH3-domain containing proteins, such as Vav1 (Madureira *et al.*, 2005;
266 Rodrigues *et al.*, 2006). Of these, P3, P4 and P5 have not been conserved in WMHV or
267 BRHV. Recent *in vivo* analysis showed that mutations of P3, P4 or P5 had no affect on the
268 establishment of, or reactivation from, splenic latency (Herskowitz *et al.*, 2008). Taken
269 together, these motifs are unlikely to be important for M2's signalling function. In a similar
270 vein, the tyrosine residues at positions 120 and 129 of M2, which have been proven to be
271 functional (Herskowitz *et al.*, 2008; Pires de Miranda *et al.*, 2008), are conserved in both
272 WMHV and BRHV, highlighting their importance for M2's signalling function.
273
274 The second most divergent protein in WMHV and MuHV4 is the virion glycoprotein gp150,
275 which is encoded by *ORF51*. It seems likely that, in addition to exhibiting extensive

differences in amino acid sequence, these proteins are predicted to be N-glycosylated differently in the two viruses (Fig. 5c). Gp150 is a major target for the host antibody response, so it is likely to be under strong selective pressure (Gillet *et al.*, 2007). However, it is not clear why this membrane glycoprotein is more variable than others encoded by the two viruses.

The most divergent protein in WMHV and MuHV4 is encoded by *ORF73* (Fig. 5d). *In vivo* analyses of an MuHV4 mutant have shown that ORF73 is essential for the establishment and maintenance of latency (Fowler *et al.*, 2003), and preliminary characterization of *ORF73* mRNAs suggests that their transcription is similar to that of KSHV *ORF73* encoding the protein LANA (Coleman *et al.*, 2005). In a similar way to KSHV-LANA, the MuHV4 ORF73 protein interacts with cellular bromodomain-containing BET proteins leading to activation of the promoters of G_1/S cyclins (Ottinger *et al.*, 2009). The reason for the sequence variability in ORF73 is not clear. However, EBV EBNA1 (the functional analogue of rhadinovirus ORF73 proteins) shows considerable variability between strains (Wrightham *et al.*, 1995), and this has consequences for EBV-associated disease (Mai *et al.*, 2007; Wang *et al.*, 2003), the function of EBNA1 as a transcriptional transactivator (Do *et al.*, 2008) and the CD8+ T cell response (Bell *et al.*, 2008).

In summary, WMHV is a novel MuHV4-like virus whose study will give further insight into gammaherpesvirus biology, especially in comparative terms alongside MuHV4.

METHODS

Cheshire herpesviruses

Isolation and growth. Eight wood mice (WM1 to WM8), a bank vole (BV1), a field vole (*Microtus agrestis*; FV1) and six house mice (HM1 to HM6) were captured in Cheshire during 2002. The animals were killed by cervical dislocation and trigeminal ganglia, lungs and spleens were removed for virus reactivation. Virus was reactivated from trigeminal ganglia by explant culture as described previously (Efstathiou *et al.*, 1986). Virus was reactivated from the spleen by using an infectious centre assay (Sunil-Chandra *et al.*, 1992). Lung tissue was homogenized and virus recovered as described previously (Stewart *et al.*, 1998). Mouse NIH3T3 cells (Todaro & Green, 1963) were used for all virus isolation experiments. Supernatants were examined as negatively stained preparations by transmission electron microscopy (TEM).

Preliminary sequence analysis. Samples were tested for the presence of herpesvirus DNA polymerase gene (DPOL) sequences by PCR. Whole-cell DNA from NIH3T3 cells was purified at 18-24 h post infection (PI) using a QIAamp DNA Mini Kit (Qiagen). PCR was carried out using the degenerate, deoxyinosine-substituted primers 5'-TGTAACTCGGTGTAYGGITTYACIGGIGT-3' and 5'-CACAGAGTCCGTRTCICCRTAIAT-3' (Ehlers *et al.*, 1999). PCR products were inserted into pCR2.1topo (Invitrogen Life Technologies) and inserts were sequenced from three individual clones per product by Lark Technologies Inc., UK. Amino acid sequences deduced from the sequences of the PCR products were compared to known herpesvirus DPOL sequences using BLAST (Altschul *et al.*, 1997).

To amplify protein-coding DNA from genes *M1*, *M2* and *M3*, the samples were subjected to PCR using primers M1-f/M1-r (5'-TCATTGAGCAGCGGCGAC-3' and 5'-GTATTCAGGCTTAGGACTG-3'; 1292 bp), M2-f/M2-r (5'-ATGGCCCCAACACCCCCAC-3' and 5'-ACTCCTCGCCCCACTCCAC-3'; 577 bp) and M3-f/M3-r (5'-CTCTGGGAGAGCGTCAG-3' and 5'-GTTACTGAGTATCAATGATCC-3'; 1251 bp),

respectively. PCR products were sequenced as described above. The sequences obtained, minus those of the primers, accounted for the entire protein-coding region of each gene but for a few codons at one or both ends.

Genome sequence analysis. Virus isolated from the WM8 spleen was plaque-purified three times from infected NIH3T3 cells overlaid with agarose, and a master stock of cell-associated virus was prepared and titrated. For the purposes of the present study, this virus was designated wood mouse herpesvirus (WMHV). WMHV was found to be primarily cell-associated in culture. To prepare virions for DNA extraction, WMHV was grown on a mouse cell line (αβSV1) deficient in the response to α/β interferon. This line was derived by first generating mouse embryonic fibroblasts (Todaro & Green, 1963) from interferon α/β receptor knockout mice (Muller *et al.*, 1994). These cells were then transformed by transfection with a plasmid expressing SV40 T antigen (pVU0) (Kalderon *et al.*, 1982) to generate an immortal cell line. The resulting cell line was found in preliminary experiments to release a much higher level of cell-free virus.

Twenty 150-cm^2 tissue culture flasks of sub-confluent αβSV1 cells were infected with WMHV at an MOI of 0.01 for 7 d. Virus DNA was then purified as described (Baldick *et al.*, 1997) and its integrity confirmed by agarose gel electrophoresis.

The DNA was sequenced at the Wellcome Trust Sanger Institute by a standard random shotgun approach to an average coverage of 12 reads per nucleotide. Tandem repeat regions in the genome were determined using the program MREPS (Kolpakov *et al.*, 2003), and the genome ends were inferred by comparison with the MuHV4 sequence (U97553; (Virgin *et al.*, 1997). The main computer programs used to analyse the sequence were: for sequence annotation, Artemis (Rutherford *et al.*, 2000), ACT (Carver *et al.*, 2005), and Sequin (NCBI); for sequence alignment, ClustalW (Thompson *et al.*, 1994) and Mafft (Katoh

& Toh, 2008); for DNA sequence analyses, GCG (Accelrys) and EMBOSS (Rice *et al.*, 2000); for amino acid sequence analysis, GCG, ExPASy (Gasteiger *et al.*, 2003), PTrans (Taylor, 1986) and Philius (Reynolds *et al.*, 2008); and for similarity searches, BLAST and FASTA and its relatives (Pearson & Lipman, 1988).

Biological characterization. The growth properties of WMHV were compared with those of MuHV4 in laboratory-bred wood mice using the procedures described (Sunil-Chandra *et al.*, 1992). All animal work was performed under UK Home Office Project Licence number 40/2483 and Personal Licence number 60/6501.

Wood mice (*Apodemus sylvaticus*) were obtained from an out-bred colony established at the Faculty of Veterinary Science, University of Liverpool (Bennett *et al.*, 1997; Feore *et al.*, 1997). This colony was obtained from Dr. J. Clarke in 1995, and was derived from captive-bred colonies that had been maintained for several decades in the Department of Zoology, University of Oxford, with only occasional introductions of new stock from the wild. Their general housing and maintenance has been described elsewhere (Clarke, 1998), and at Liverpool they are maintained under semi-barrier conditions. The Liverpool colony has suffered no clinical disease, and, although not specified pathogen free (SPF) in the sense used for most laboratory rodents, all samples tested for the major infections of laboratory rodents have so far been negative. Of particular relevance to this study, no evidence of MuHV4 infection has been detected by serology and PCR analysis (Blasdell *et al.*, 2003). Both male and female wood mice of 5 – 8 weeks of age were used. They were infected intranasally with 4×10^5 PFU of virus, and the lungs, spleens and bronchial lymph nodes were harvested at various times PI. Lung tissue was homogenized, and the lysate was freeze-thawed three times and used in plaque assays. Leukocytes were purified from the spleens and counted, and virus reactivation was monitored using an infective centre assay. Tissues from infected wood mice were routinely processed for histopathological examination, including immunohistology.

382

383 **Brest herpesvirus**

384 ***Isolation and growth.*** The herpesvirus (Brest/AN711) isolated from a white-toothed shrew
385 (Chastel *et al.*, 1994) was grown and titrated on baby hamster kidney (BHK) cells as
386 described (Bridgeman *et al.*, 2001). For the purposes of the present study, this virus was
387 named Brest herpesvirus (BRHV). To prepare viral DNA, confluent monolayers of cells in
388 175-cm^2 flasks were infected at an MOI of 0.01. When CPE was complete at approximately
389 4 d PI, virions were purified from the medium by Ficoll gradient ultracentrifugation as
390 described (Lopes *et al.*, 2004). Banded virus was diluted with PBS to a total volume of 30 ml,
391 and pelleted at 30000 x *g* for 90 min. The pelleted virus was resuspended in TE buffer
392 containing 0.5 % (w/v) SDS and 50 μg ml^{-1} proteinase K. The mixture was incubated
393 overnight at 37 ºC and extracted with phenol, and the DNA precipitated in ethanol and
394 dissolved in a small volume of TE, as described above.

395

396 ***Preliminary sequence analysis.*** Initial cloning involved the generation of a small library of
397 bacteriophage M13 recombinants containing BRHV AluI fragments, using standard methods.
398 The inserts in three recombinants were sequenced, and found by BLAST similarity search to
399 be most closely related to the MuHV4 genome. Respectively, the insert sizes were 148, 145
400 and 156 bp and exhibited 89.2, 96.6 and 90.4 % nucleotide sequence identity to ORF18,
401 ORF31 and ORF60.

402

403 ***Partial genome sequence analysis.*** A cosmid library was generated from BRHV DNA as
404 described (Cunningham & Davison, 1993). Three overlapping cosmid clones constituting
405 approximately 70 kbp of the genome were sequenced, the first by a standard random
406 shotgun approach, and the other two by iterative primer-walking on both strands, based
407 initially on data generated from the first cosmid or arising from the preliminary sequence
408 analysis described above. The computer programs used for analysis are listed above.

ACKNOWLEDGEMENTS

This work was funded by the Medical Research Council (United Kingdom), the Wellcome Trust, U.S. Public Health Service grant CA090208, and the Penn State Hershey Cancer Institute. JPS was funded by a Royal Society (London) University Research Fellowship. Initial isolation experiments were funded by a Royal Society (London) Summer Studentship to DJH. TEM was performed by Brian Getty (School of Infection and Host Defence, Liverpool), and histology and immunohistology by the Histology Laboratory, Veterinary Laboratory Services, Faculty of Veterinary Science, University of Liverpool.

REFERENCES

Altschul, S. F., Madden, T. L., Schaffer, A. A., Zhang, J., Zhang, Z., Miller, W. & Lipman, D. J. (1997). Gapped BLAST and PSI-BLAST: a new generation of protein database search programs. *Nucleic Acids Res* **25**, 3389-3402.

Baldick, C. J., Jr., Marchini, A., Patterson, C. E. & Shenk, T. (1997). Human cytomegalovirus tegument protein pp71 (ppUL82) enhances the infectivity of viral DNA and accelerates the infectious cycle. *J Virol* **71**, 4400-4408.

Bell, M. J., Brennan, R., Miles, J. J., Moss, D. J., Burrows, J. M. & Burrows, S. R. (2008). Widespread sequence variation in Epstein-Barr virus nuclear antigen 1 influences the antiviral T cell response. *J Infect Dis* **197**, 1594-1597.

Bennett, M., Crouch, A. J., Begon, M., Duffy, B., Feore, S., Gaskell, R. M., Kelly, D. F., McCracken, C. M., Vicary, L. & Baxby, D. (1997). Cowpox in British voles and mice. *J Comp Pathol* **116**, 35-44.

Blasdell, K., McCracken, C., Morris, A., Nash, A. A., Begon, M., Bennett, M. & Stewart, J. P. (2003). The wood mouse is a natural host for Murid herpesvirus 4. *J Gen Virol* **84**, 111-113.

Blaskovic, D., Stancekova, M., Svobodova, J. & Mistrikova, J. (1980). Isolation of five strains of herpesviruses from two species of free living small rodents. *Acta Virol* **24**, 468.

Bowden, R. J., Simas, J. P., Davis, A. J. & Efstathiou, S. (1997). Murine gammaherpesvirus 68 encodes tRNA-like sequences which are expressed during latency. *J Gen Virol* **78**, 1675-1687.

Bridgeman, A., Stevenson, P. G., Simas, J. P. & Efstathiou, S. (2001). A secreted chemokine binding protein encoded by murine gammaherpesvirus- 68 is necessary for the establishment of a normal latent load. *J Exp Med* **194**, 301-312.

Carver, T. J., Rutherford, K. M., Berriman, M., Rajandream, M. A., Barrell, B. G. & Parkhill, J. (2005). ACT: the Artemis Comparison Tool. *Bioinformatics* **21**, 3422-3423.

Chastel, C., Beaucournu, J. P., Chastel, O., Legrand, M. C. & Le Goff, F. (1994). A herpesvirus from an European shrew (Crocidura russula). *Acta Virol* **38**, 309.

Ciampor, F., Stancekova, M. & Blaskovic, D. (1981). Electron microscopy of rabbit embryo fibroblasts infected with herpesvirus isolates from Clethrionomys glareolus and Apodemus flavicollis. *Acta Virol* **25**, 101-107.

Clambey, E. T., Virgin, H. W. t. & Speck, S. H. (2002). Characterization of a spontaneous 9.5-kilobase-deletion mutant of murine gammaherpesvirus 68 reveals tissue-specific genetic requirements for latency. *J Virol* **76**, 6532-6544.

Clarke, J. R. (1998). Voles. In *UFAW Handbook on the Care and Management of Laboratory Animals*. Edited by T. B. Poole. Oxford: Blackwell Scientific.

Coleman, H. M., Efstathiou, S. & Stevenson, P. G. (2005). Transcription of the murine gammaherpesvirus 68 ORF73 from promoters in the viral terminal repeats. *J Gen Virol* **86**, 561-574.

Cunningham, C. & Davison, A. J. (1993). A cosmid-based system for constructing mutants of herpes simplex virus type 1. *Virology* **197**, 116-124.

Davison, A. J., Eberle, R., Ehlers, B., Hayward, G. S., McGeoch, D. J., Minson, A. C., Pellett, P. E., Roizman, B., Studdert, M. J. & Thiry, E. (2009). The order Herpesvirales. *Arch Virol* **154**, 171-177.

Do, N. V., Ingemar, E., Phi, P. T., Jenny, A., Chinh, T. T., Zeng, Y. & Hu, L. (2008). A major EBNA1 variant from Asian EBV isolates shows enhanced transcriptional activity compared to prototype B95.8. *Virus Res* **132**, 15-24.

Ebrahimi, B., Dutia, B. M., Roberts, K. L., Garcia-Ramirez, J. J., Dickinson, P., Stewart, J. P., Ghazal, P., Roy, D. J. & Nash, A. A. (2003). Transcriptome profile of murine gammaherpesvirus-68 lytic infection. *J Gen Virol* **84**, 99-109.

Efstathiou, S., Ho, Y. M., Hall, S., Styles, C. J., Scott, S. D. & Gompels, U. A. (1990). Murine herpesvirus 68 is genetically related to the gammaherpesviruses Epstein-Barr virus and herpesvirus saimiri. *J Gen Virol* **71**, 1365-1372.

Efstathiou, S., Minson, A. C., Field, H. J., Anderson, J. R. & Wildy, P. (1986). Detection of herpes simplex virus-specific DNA sequences in latently infected mice and in humans. *J Virol* **57**, 446-455.

Ehlers, B., Borchers, K., Grund, C., Frolich, K., Ludwig, H. & Buhk, H. J. (1999). Detection of new DNA polymerase genes of known and potentially novel herpesviruses by PCR with degenerate and deoxyinosine-substituted primers. *Virus Genes* **18**, 211-220.

Ehlers, B., Kuchler, J., Yasmum, N., Dural, G., Voigt, S., Schmidt-Chanasit, J., Jakel, T., Matuschka, F. R., Richter, D., Essbauer, S., Hughes, D. J., Summers, C., Bennett, M., Stewart, J. P. & Ulrich, R. G. (2007). Identification of novel rodent herpesviruses, including the first gammaherpesvirus of Mus musculus. *J Virol* **81**, 8091-8100.

Evans, A. G., Moorman, N. J., Willer, D. O. & Speck, S. H. (2006). The M4 gene of gammaHV68 encodes a secreted glycoprotein and is required for the efficient establishment of splenic latency. *Virology* **344**, 520-531.

Evans, A. G., Moser, J. M., Krug, L. T., Pozharskaya, V., Mora, A. L. & Speck, S. H. (2008). A gammaherpesvirus-secreted activator of Vbeta4+ CD8+ T cells regulates chronic infection and immunopathology. *J Exp Med* **205**, 669-684.

Feore, S. M., Bennett, M., Chantrey, J., Jones, T., Baxby, D. & Begon, M. (1997). The effect of cowpox virus infection on fecundity in bank voles and wood mice. *Proceedings of the Royal Society of London, Series B - Biological Sciences* **264**, 1457-1461.

Fowler, P., Marques, S., Simas, J. P. & Efstathiou, S. (2003). ORF73 of murine herpesvirus-68 is critical for the establishment and maintenance of latency. *J Virol* **84**, 3405-3416.

Gasteiger, E., Gattiker, A., Hoogland, C., Ivanyi, I., Appel, R. D. & Bairoch, A. (2003). ExPASy: The proteomics server for in-depth protein knowledge and analysis. *Nucleic Acids Res* **31**, 3784-3788.

Geere, H. M., Ligertwood, Y., Templeton, K. M., Bennet, I., Gangadharan, B., Rhind, S. M., Nash, A. A. & Dutia, B. M. (2006). The M4 gene of murine gammaherpesvirus 68 modulates latent infection. *J Gen Virol* **87**, 803-807.

Gillet, L., May, J. S., Colaco, S. & Stevenson, P. G. (2007). The murine gammaherpesvirus-68 gp150 acts as an immunogenic decoy to limit virion neutralization. *PLoS One* **2**, e705.

Hamelin, C. & Lussier, G. (1992). Characterization of the DNA of rodent herpesviruses by restriction endonuclease analysis and hybridization. *Lab Anim Sci* **42**, 142-145.

Herskowitz, J. H., Siegel, A. M., Jacoby, M. A. & Speck, S. H. (2008). Systematic mutagenesis of the murine gammaherpesvirus 68 M2 protein identifies domains important for chronic infection. *J Virol* **82**, 3295-3310.

Husain, S. M., Usherwood, E. J., Dyson, H., Coleclough, C., Coppola, M. A., Woodland, D. L., Blackman, M. A., Stewart, J. P. & Sample, J. T. (1999). Murine gammaherpesvirus M2 gene is latency-associated and its protein a target for CD8(+) T lymphocytes. *Proc Natl Acad Sci USA* **96**, 7508-7513.

Jacoby, M. A., Virgin, H. W. t. & Speck, S. H. (2002). Disruption of the M2 gene of murine gammaherpesvirus 68 alters splenic latency following intranasal, but not intraperitoneal, inoculation. *J Virol* **76**, 1790-1801.

Kalderon, D., Oostra, B. A., Ely, B. K. & Smith, A. E. (1982). Deletion loop mutagenesis: a novel method for the construction of point mutations using deletion mutants. *Nucleic Acids Res* **10**, 5161-5171.

Katoh, K. & Toh, H. (2008). Recent developments in the MAFFT multiple sequence alignment program. *Brief Bioinform* **9**, 286-298.

Kolpakov, R., Bana, G. & Kucherov, G. (2003). mreps: Efficient and flexible detection of tandem repeats in DNA. *Nucleic Acids Res* **31**, 3672-3678.

Lopes, F. B., Colaco, S., May, J. S. & Stevenson, P. G. (2004). Characterization of murine gammaherpesvirus 68 glycoprotein B. *J Virol* **78**, 13370-13375.

Macakova, K., Matis, J., Rezuchova, I., Kudela, O., Raslova, H. & Kudelova, M. (2003). Murine gammaherpesvirus (MHV) M7 gene encoding glycoprotein 150 (gp150): difference in the sequence between 72 and 68 strains. *Virus Genes* **26**, 89-95.

Macrae, A. I., Dutia, B. M., Milligan, S., Brownstein, D. G., Allen, D. J., Mistrikova, J., Davison, A. J., Nash, A. A. & Stewart, J. P. (2001). Analysis of a Novel Strain of Murine Gammaherpesvirus Reveals a Genomic Locus Important for Acute Pathogenesis. *J Virol* **75**, 5315-5327.

Macrae, A. I., Usherwood, E. J., Husain, S. M., Flano, E., Kim, I. J., Woodland, D. L., Nash, A. A., Blackman, M. A., Sample, J. T. & Stewart, J. P. (2003). Murid herpesvirus 4 strain 68 M2 protein is a B-cell-associated antigen important for latency but not lymphocytosis. *J Virol* **77**, 9700-9709.

Madureira, P. A., Matos, P., Soeiro, I., Dixon, L. K., Simas, J. P. & Lam, E. W. (2005). Murine gamma-herpesvirus 68 latency protein M2 binds to Vav signaling proteins and inhibits B-cell receptor-induced cell cycle arrest and apoptosis in WEHI-231 B cells. *J Biol Chem* **280**, 37310-37318.

Mai, S. J., Ooka, T., Li, D. J., Zeng, M. S., Jiang, R. C., Yu, X. J., Zhang, R. H., Chen, S. P. & Zeng, Y. X. (2007). Functional advantage of NPC-related V-val subtype of Epstein-Barr virus nuclear antigen 1 compared with prototype in epithelial cell line. *Oncol Rep* **17**, 141-146.

Marques, S., Alenquer, M., Stevenson, P. G. & Simas, J. P. (2008). A single CD8+ T cell epitope sets the long-term latent load of a murid herpesvirus. *PLoS Pathog* **4**, e1000177.

McGeoch, D. J., Gatherer, D. & Dolan, A. (2005). On phylogenetic relationships among major lineages of the Gammaherpesvirinae. *J Gen Virol* **86**, 307-316.

McGeoch, D. J., Rixon, F. J. & Davison, A. J. (2006). Topics in herpesvirus genomics and evolution. *Virus Res* **117**, 90-104.

Mistríková, J., Raslova, H., Mrmusova, M. & Kudelova, M. (2000). A murine gammaherpesvirus. *Acta Virol* **44**, 211-226.

Muller, U., Steinhoff, U., Reis, L. F., Hemmi, S., Pavlovic, J., Zinkernagel, R. M. & Aguet, M. (1994). Functional role of type I and type II interferons in antiviral defense. *Science* **264**, 1918-1921.

Nash, A. A., Dutia, B. M., Stewart, J. P. & Davison, A. J. (2001). Natural history of murine gamma-herpesvirus infection. *Philos Trans R Soc Lond B Biol Sci* **356**, 569-579.

Oda, W., Mistrikova, J., Stancekova, M., Dutia, B. M., Nash, A. A., Takahata, H., Jin, Z., Oka, T. & Hayashi, K. (2005). Analysis of genomic homology of murine gammaherpesvirus (MHV)-72 to MHV-68 and impact of MHV-72 on the survival and tumorigenesis in the MHV-72-infected CB17 scid/scid and CB17+/+ mice. *Pathol Int* **55**, 558-568.

Ottinger, M., Pliquet, D., Christalla, T., Frank, R., Stewart, J. P. & Schulz, T. F. (2009). The interaction of the gammaherpesvirus 68 orf73 protein with cellular BET proteins affects the activation of cell cycle promoters. *J Virol* **83**, 4423-4434.

Parry, C. M., Simas, J. P., Smith, V. P., Stewart, C. A., Minson, A. C., Efstathiou, S. & Alcami, A. (2000). A broad spectrum secreted chemokine binding protein encoded by a herpesvirus. *J Exp Med* **191**, 573-578.

Pearson, W. R. & Lipman, D. J. (1988). Improved tools for biological sequence comparison. *Proc Natl Acad Sci USA* **85**, 2444-2448.

Pfeffer, S., Zavolan, M., Grasser, F. A., Chien, M., Russo, J. J., Ju, J., John, B., Enright, A. J., Marks, D., Sander, C. & Tuschl, T. (2004). Identification of virus-encoded microRNAs. *Science* **304**, 734-736.

Pires de Miranda, M., Alenquer, M., Marques, S., Rodrigues, L., Lopes, F., Bustelo, X. R. & Simas, J. P. (2008). The Gammaherpesvirus m2 protein manipulates the Fyn/Vav pathway through a multidocking mechanism of assembly. *PLoS One* **3**, e1654.

Raslova, H., Matis, J., Rezuchova, I., Macakova, K., Berebbi, M. & Kudelova, M. (2000). The bystander effect mediated by the new murine gammaherpesvirus 72-- thymidine kinase/5'-fluoro-2'-deoxyuridine (MHV72-TK/5-FUdR) system in vitro [In Process Citation]. *Antivir Chem Chemother* **11**, 273-282.

Reynolds, S. M., Kall, L., Riffle, M. E., Bilmes, J. A. & Noble, W. S. (2008). Transmembrane topology and signal peptide prediction using dynamic bayesian networks. *PLoS Comput Biol* **4**, e1000213.

Rice, P., Longden, I. & Bleasby, A. (2000). EMBOSS: the European Molecular Biology Open Software Suite. *Trends Genet* **16**, 276-277.

Rodrigues, L., Pires de Miranda, M., Caloca, M. J., Bustelo, X. R. & Simas, J. P. (2006). Activation of Vav by the gammaherpesvirus M2 protein contributes to the establishment of viral latency in B lymphocytes. *J Virol* **80**, 6123-6135.

Rutherford, K., Parkhill, J., Crook, J., Horsnell, T., Rice, P., Rajandream, M. A. & Barrell, B. (2000). Artemis: sequence visualization and annotation. *Bioinformatics* **16**, 944-945.

Simas, J. P., Marques, S., Bridgeman, A., Efstathiou, S. & Adler, H. (2004). The M2 gene product of murine gammaherpesvirus 68 is required for efficient colonization of splenic follicles but is not necessary for expansion of latently infected germinal centre B cells. *J Gen Virol* **85**, 2789-2797.

Simas, J. P., Swann, D., Bowden, R. & Efstathiou, S. (1999). Analysis of murine gammaherpesvirus-68 transcription during lytic and latent infection. *J Gen Virol* **80**, 75-82.

Stewart, J. P., Usherwood, E. J., Ross, A., Dyson, H. & Nash, T. (1998). Lung epithelial cells are a major site of murine gammaherpesvirus persistence. *J Exp Med* **187**, 1941-1951.

Sunil-Chandra, N. P., Efstathiou, S., Arno, J. & Nash, A. A. (1992). Virological and pathological features of mice infected with murine gamma-herpesvirus 68. *J Gen Virol* **73**, 2347-2356.

Svobodova, J., Blaskovic, D. & Mistrikova, J. (1982). Growth characteristics of herpesviruses isolated from free living small rodents. *Acta Virol* **26**, 256-263.

Taylor, P. (1986). A computer program for translating DNA sequences into protein. *Nucleic Acids Res* **14**, 437-441.

Thompson, J. D., Higgins, D. G. & Gibson, T. J. (1994). CLUSTAL W: improving the sensitivity of progressive multiple sequence alignment through sequence weighting, positions-specific gap penalties and weight matrix choice. *Nuleic Acids Research* **22**, 4673-4680.

Todaro, G. J. & Green, H. (1963). Quantitative studies of the growth of mouse embryo cells in culture and their development into established lines. *J Cell Biol* **17**, 299-313.

Usherwood, E. J., Roy, D. J., Ward, K., Surman, S. L., Dutia, B. M., Blackman, M. A., Stewart, J. P. & Woodland, D. L. (2000). Control of gammaherpesvirus latency by latent antigen-specific CD8(+) T cells. *J Exp Med* **192**, 943-952.

van Berkel, V., Barrett, J., Tiffany, H. L., Fremont, D. H., Murphy, P. M., McFadden, G., Speck, S. H. & Virgin, H. W. (2000). Identification of a gammaherpesvirus selective chemokine binding protein that inhibits chemokine action. *J Virol* **74**, 6741-6747.

van Berkel, V., Levine, B., Kapadia, S. B., Goldman, J. E., Speck, S. H. & Virgin, H. W. t. (2002). Critical role for a high-affinity chemokine-binding protein in gamma-herpesvirus-induced lethal meningitis. *J Clin Invest* **109**, 905-914.

van Berkel, V., Preiter, K., Virgin, H. W. & Speck, S. H. (1999). Identification and initial characterization of the murine gammaherpesvirus 68 gene M3, encoding an abundantly secreted protein. *J Virol* **73**, 4524-4529.

Virgin, H. W., Latreille, P., Wamsley, P., Hallsworth, K., Weck, K. E., Dal Canto, A. J. & Speck, S. H. (1997). Complete sequence and genomic analysis of murine gammaherpesvirus 68. *J Virol* **71**, 5894-5904.

Virgin, H. W., Presti, R. M., Li, X. Y., Liu, C. & Speck, S. H. (1999). Three distinct regions of the murine gammaherpesvirus 68 genome are transcriptionally active in latently infected mice. *J Virol* **73**, 2321-2332.

Wang, J. T., Sheeng, T. S., Su, I. J., Chen, J. Y. & Chen, M. R. (2003). EBNA-1 sequence variations reflect active EBV replication and disease status or quiescent latency in lymphocytes. *J Med Virol* **69**, 417-425.

Wrightham, M. N., Stewart, J. P., Janjua, N. J., Pepper, S. D., Sample, C., Rooney, C. M. & Arrand, J. R. (1995). Antigenic and sequence variation in the C-terminal unique domain of the Epstein-Barr virus nuclear antigen EBNA-1. *Virology* **208**, 521-530.

Table 1. Isolation of herpesviruses from free-living rodents in Cheshire.

Animal*	Tissues harvested†	Tissues yielding CPE†	Herpesvirus particles‡
WM1	TG, S, L	TG, S	+
WM2	TG, S, L	S	+
WM3	TG, S, L	–	–
WM4	TG, S, L	–	–
WM5	TG, S, L	–	–
WM6	TG, S, L	–	–
WM7	TG, S, L	TG	+
WM8	TG, S, L	TG, S	+
BV1	TG, S, L	–	–
FV1	S, L	S	+
HM1	TG, S, L	–	–
HM2	TG, S, L	–	–
HM3	TG, S, L	–	–
HM4	TG, S, L	S	+
HM5	TG, S, L	–	–
HM6	TG, S, L	–	–

* WM, wood mouse; BV, bank vole; FV, field vole; HM, house mouse; followed by a number for each animal.
† TG, trigeminal ganglia; S, spleen; L, lungs; –, no CPE.
‡ +, particles observed by EM; –, particles not observed by Transmission Electron Microscopy on negatively stained preparations.

FIGURE LEGENDS

Fig. 1. PCR amplification of the coding regions of genes (a) *M1*, (b) *M2* and (c) *M3* from viruses isolated from FV1, WM1, WM2, WM7 and WM8, in comparison with MuHV4. TG, trigeminal ganglia; S, spleen.

Fig. 2. Variation between the genome sequences of WMHV and MuHV4. The lower part of the panels represent the genome, commencing in the first panel at the start of U and ending in the last panel with one copy of TR, which is shown in a thicker format. Protein-coding regions are depicted by shaded arrows, with connecting introns indicated by white horizontal bars, and genes encoding the tRNA-like genes (1-8) are shown as arrowheads. Internal tandem repeats are represented by black horizontal bars. The upper part of each panel shows the nucleotide divergence (nd) calculated for a 100-nucleotide window, shifted by increments of 3 nucleotides. A nucleotide position was counted as divergent if it differed between the two sequences; insertions or deletions were not scored.

Fig. 3. Divergence between the amino acid sequences of predicted protein-coding regions in WMHV, BRHV and MuHV4. The histogram illustrates sequence divergence (% non-identity) between the amino acid sequence of predicted protein-coding regions in WMHV and MuHV4 (grey bars, all coding regions) and BRHV and WMHV (black bars, coding regions to *ORF52*)

Fig. 4. Alignments of the predicted nucleotide sequences of the *tRNA*-like genes and *miRNAs* from MuHV4 and WMHV. A diagrammatic representation of the genomic region showing the relative positions of these non-coding RNAs is shown at the top. The positions of the *M1-M3* ORFs and viral *tRNA*-like transcripts (t1–t8) are shown by arrows. The positions of the *miRNAs* (miR-M1-1 through M1-9) derived from primary transcripts of the *tRNA*-like RNAs are shown by vertical lines. Sequence alignments of the *tRNA*/*miRNA* transcripts are shown below. The sections processed to generate the *tRNA*-like molecues are shaded grey and pre-miRNAs are shaded blue. The positions of the A and B box of the RNA Polymerase III promoters are shown by open boxes, as are the positions of the processed *miRNAs*. The positions of the anti-codons in the *tRNAs* are shown in blue type. Differences between MuHV4 and WMHV are shown in red type. Data for MuHV4 are from (Bowden *et al.*, 1997) and (Pfeffer *et al.*, 2004).

Fig. 5. Alignments of the predicted amino acid sequences of (a) M1, M3 and M4, (b) M2, (c) ORF51, and (d) ORF73. Each individual alignment consists of the sequences from MuHV4, WMHV and BRHV, with residues that differ from the consensus (or from each other in the case of ORF73) shaded grey. In (a), the alignments for M1, M3 and M4 are aligned with each other because these three proteins are related via the residues in bold type; each sequence contains a predicted signal peptide (lower case). In (b), the positions of PXXP motifs (P1–P9), tyrosine residues 120 and 129 and the CD8 CTL epitope (CTL) are indicated above the M2 sequence. In (c), the bold residues indicate potential N-linked glycosylation sites in gp150 encoded by *ORF51*. In (d), the positions of the Brd4- and Brd2-interacting domains of the ORF73 protein are shown above the sequences.

Fig. 6. Virological analyses of WMHV infection of wood mice. Wood mice (three per time-point) were infected intranasally with 4 x 10^5 PFU of MuHV4 or WMHV. Bars represent standard deviation from the mean; the asterisk represents statistically significant differences between species (p<0.05). (a) Infectious virus recovered from the lung at 7 and 14 d PI. Titres were measured by plaque assay on NIH3T3 cells. (b) Mean leukocyte numbers per spleen. (c) Infective centre assay of the level of latency in splenocytes. Infectious virus titres in the samples were analysed in parallel and were subtracted from the total infectious centres.

Fig. 7. Cellular response to WMHV and MuHV4 infection in the lungs of wood mice at 14 d PI. (a & b), Infection with MuHV4; (a) Intense peribronchial focal lymphocyte infiltration with evidence of lymphatic follicle formation (F). B, bronchiole. HE stain. Bar = 50 μm. (b) Focal perivascular B cell infiltration with lymphatic follicle formation (F). A, artery. Staining for the B cell marker CD45R, avidin biotin peroxidase complex method, Papanicolaou's haematoxylin counterstain. Bar = 20 μM. (c & d) Infection with WMHV; (c) Moderate peribronchiolar focal lymphocyte infiltration (arrows). B, bronchiole. HE stain. Bar = 20 μm. (d) Artery with focal B cell-dominated (CD45R-positive) perivascular lymphocyte infiltration (arrows). There is evidence of B cell rolling and emigration (arrowheads). Bar = 20 μm.

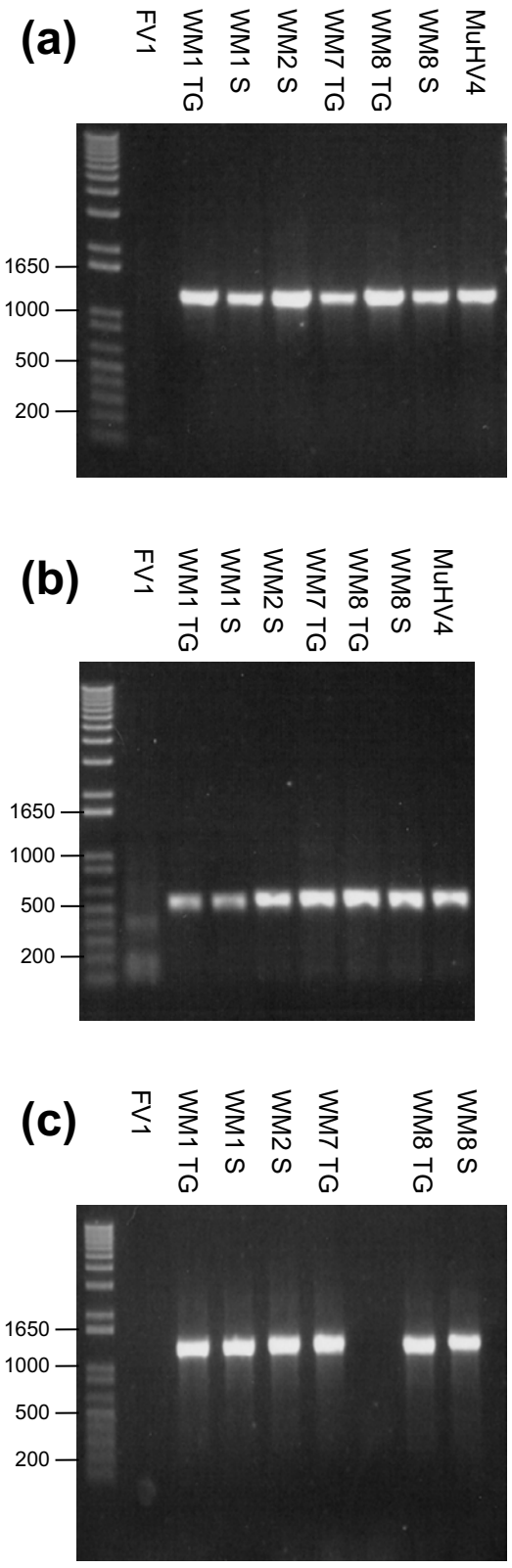
(a)
FV1
WM1 TG
WM1 S
WM2 S
WM7 TG
WM8 TG
WM8 S
MuHV4
1650
1000
500
200
(b)
FV1
WM1 TG
WM1 S
WM2 S
WM7 TG
WM8 TG
WM8 S
MuHV4
1650
1000
500
200
(c)
FV1
WM1 TG
WM1 S
WM2 S
WM7 TG
WM8 TG
WM8 S
1650
1000
500
200

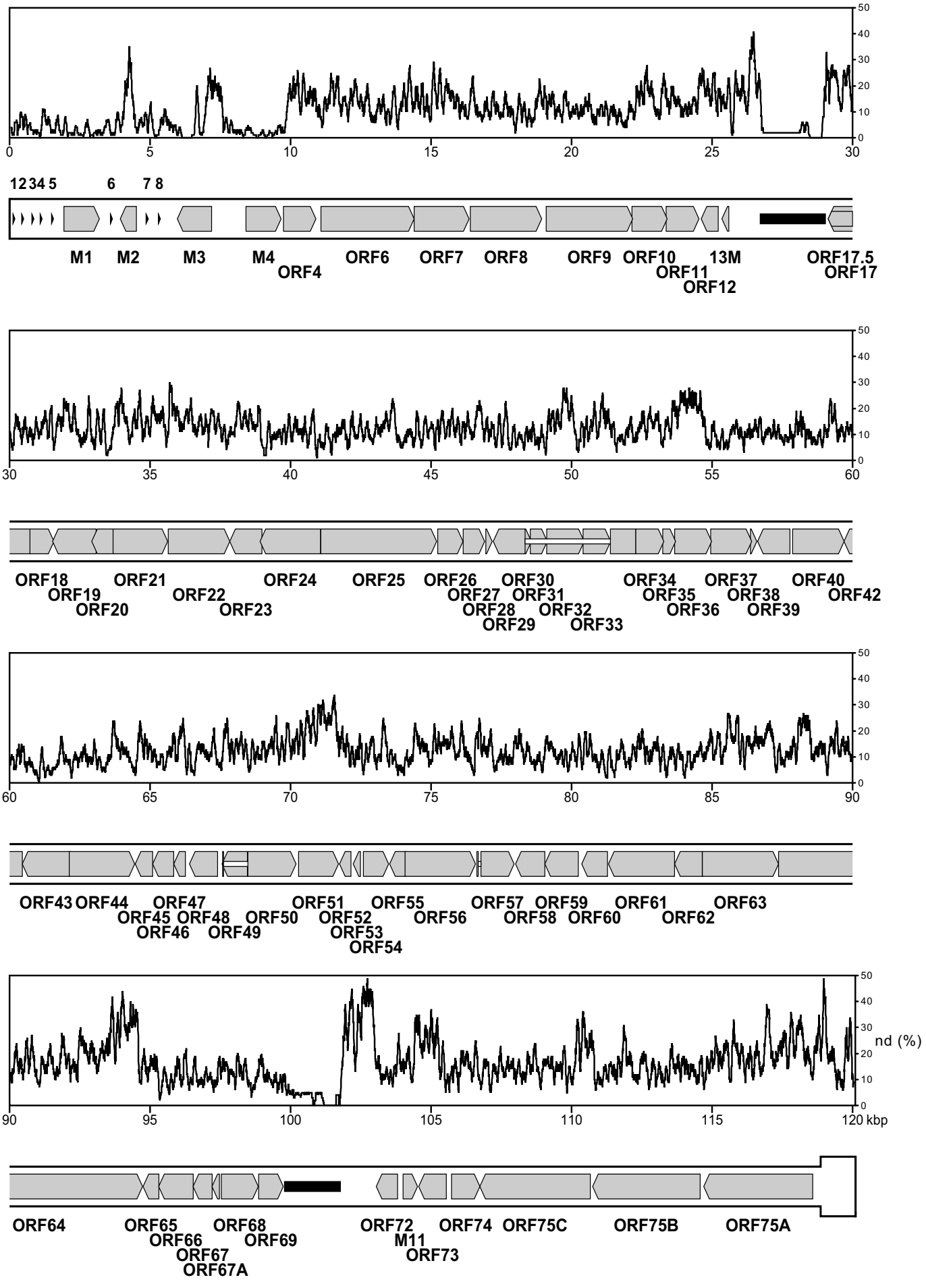
0 5 10 15 20 25 30
0 10 20 30 40 50
12345 6 7 8
M1 M2 M3 M4 ORF4 ORF6 ORF7 ORF8 ORF9 ORF10 ORF11 ORF12 13M ORF17.5 ORF17
30 35 40 45 50 55 60
ORF18 ORF19 ORF20 ORF21 ORF22 ORF23 ORF24 ORF25 ORF26 ORF27 ORF28 ORF29 ORF30 ORF31 ORF32 ORF33 ORF34 ORF35 ORF36 ORF37 ORF38 ORF39 ORF40 ORF42
60 65 70 75 80 85 90
ORF43 ORF44 ORF45 ORF46 ORF47 ORF48 ORF49 ORF50 ORF51 ORF52 ORF53 ORF54 ORF55 ORF56 ORF57 ORF58 ORF59 ORF60 ORF61 ORF62 ORF63
90 95 100 105 110 115 120 kbp
nd (%)
ORF64 ORF65 ORF66 ORF67 ORF67A ORF68 ORF69 ORF72 M11 ORF73 ORF74 ORF75C ORF75B ORF75A

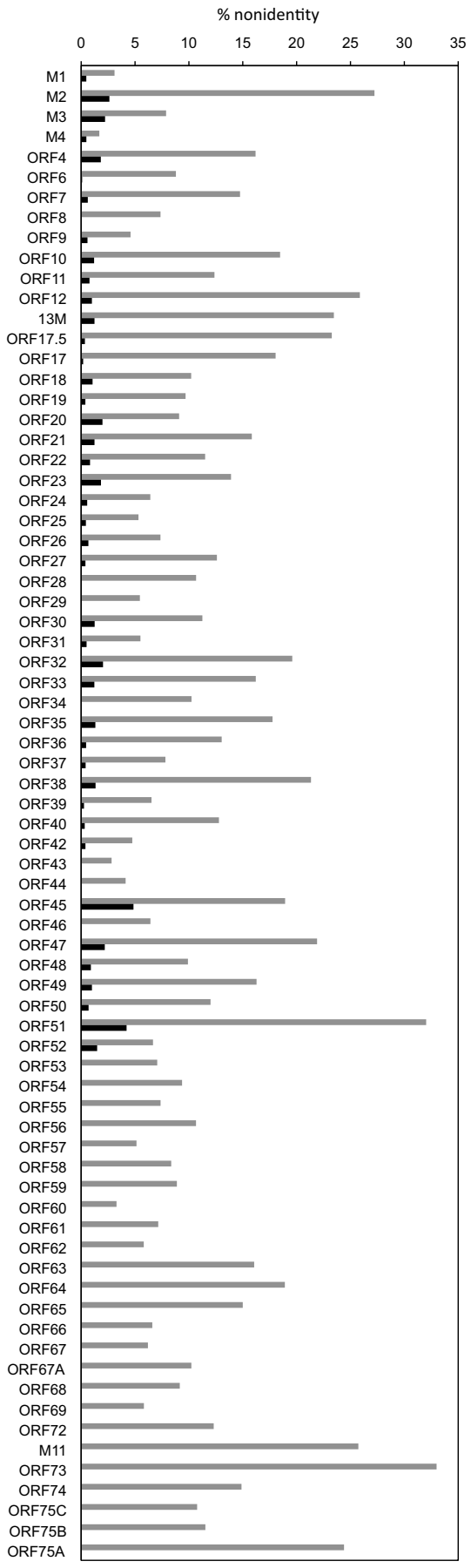
% nonidentity
0
5
10
15
20
25
30
35
M1
M2
M3
M4
ORF4
ORF6
ORF7
ORF8
ORF9
ORF10
ORF11
ORF12
13M
ORF17.5
ORF17
ORF18
ORF19
ORF20
ORF21
ORF22
ORF23
ORF24
ORF25
ORF26
ORF27
ORF28
ORF29
ORF30
ORF31
ORF32
ORF33
ORF34
ORF35
ORF36
ORF37
ORF38
ORF39
ORF40
ORF42
ORF43
ORF44
ORF45
ORF46
ORF47
ORF48
ORF49
ORF50
ORF51
ORF52
ORF53
ORF54
ORF55
ORF56
ORF57
ORF58
ORF59
ORF60
ORF61
ORF62
ORF63
ORF64
ORF65
ORF66
ORF67
ORF67A
ORF68
ORF69
ORF72
M11
ORF73
ORF74
ORF75C
ORF75B
ORF75A

Hughes et al Fig. 4

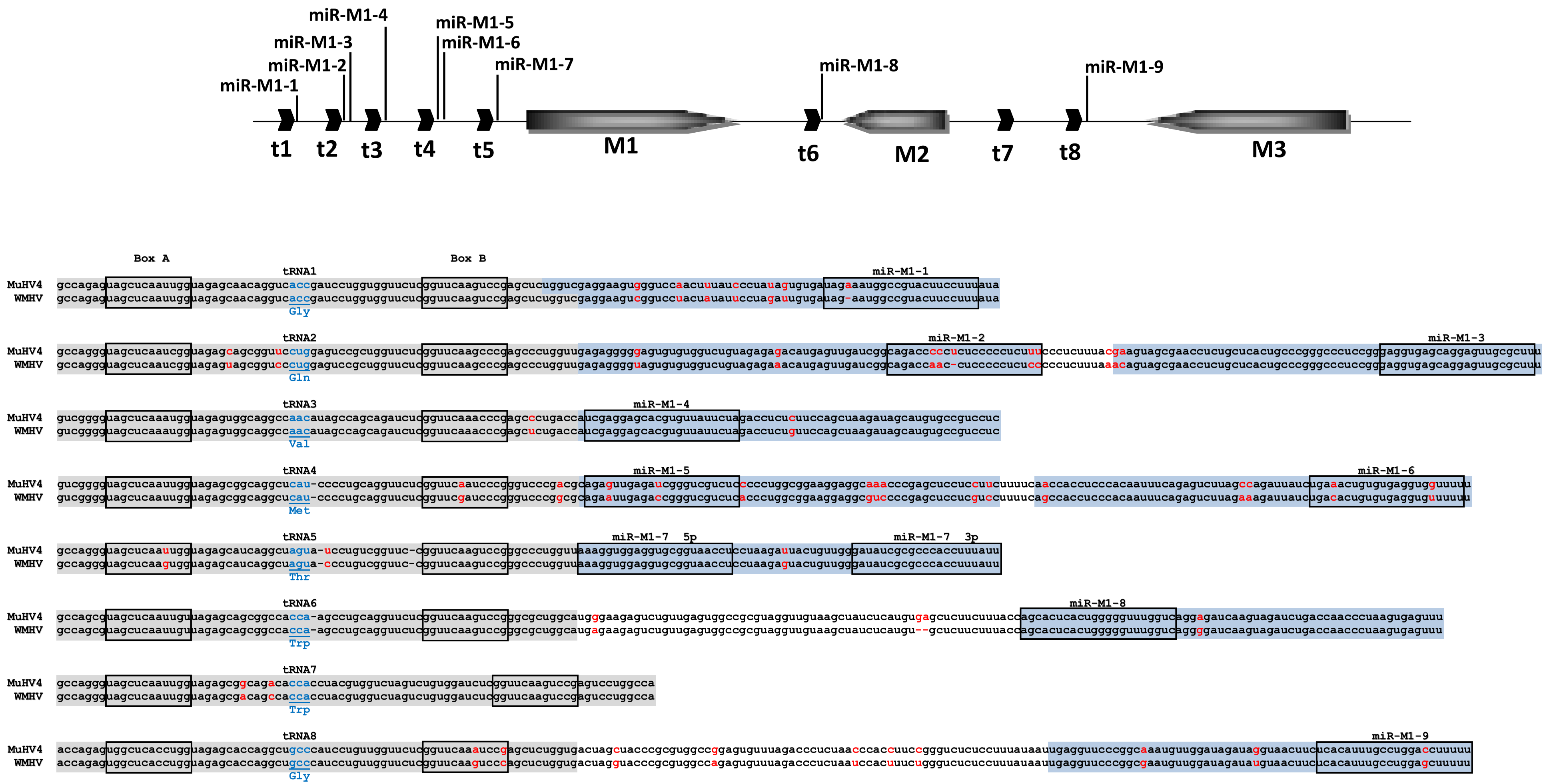

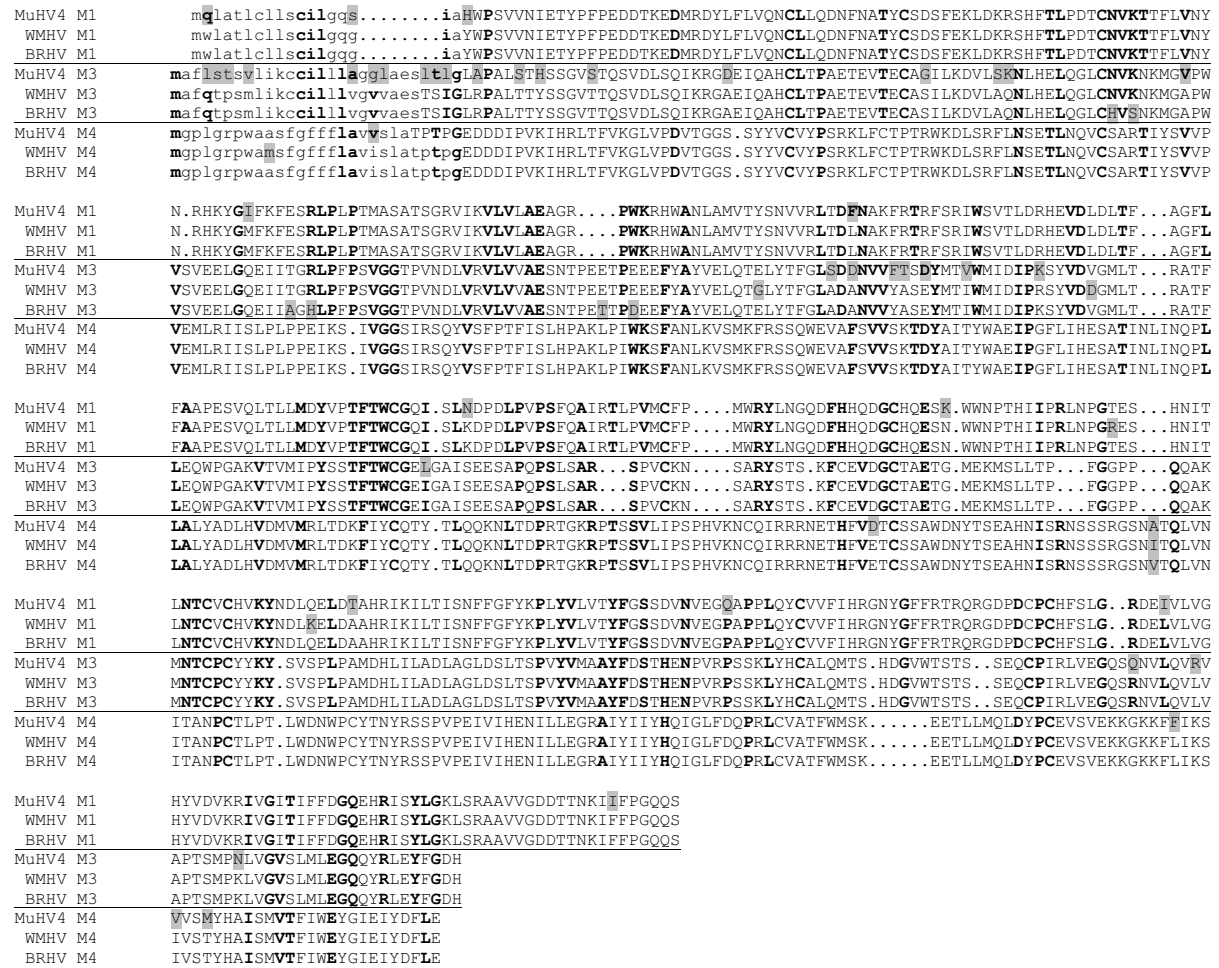
(a)
MuHV4 M1
WMHV M1
BRHV M1
MuHV4 M3
WMHV M3
BRHV M3
MuHV4 M4
WMHV M4
BRHV M4

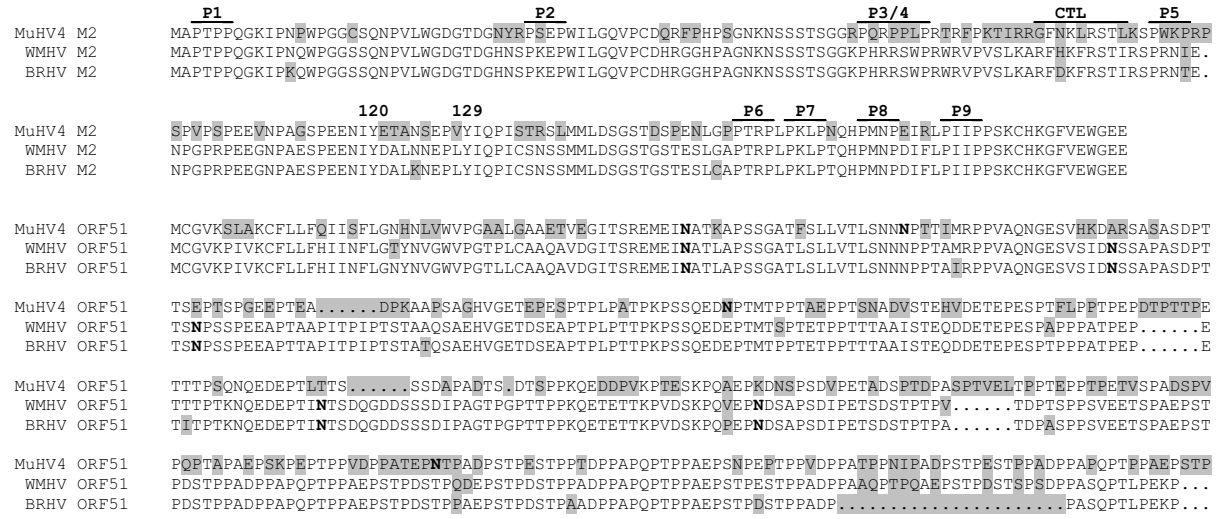
(b)
P1
P2
P3/4
CTL
P5
120
129
P6
P7
P8
P9
MuHV4 M2
WMHV M2
BRHV M2

(c)
MuHV4 ORF51
WMHV ORF51
BRHV ORF51

(d)
Brd4
Brd2
MuHV4 ORF73
WMHV ORF73

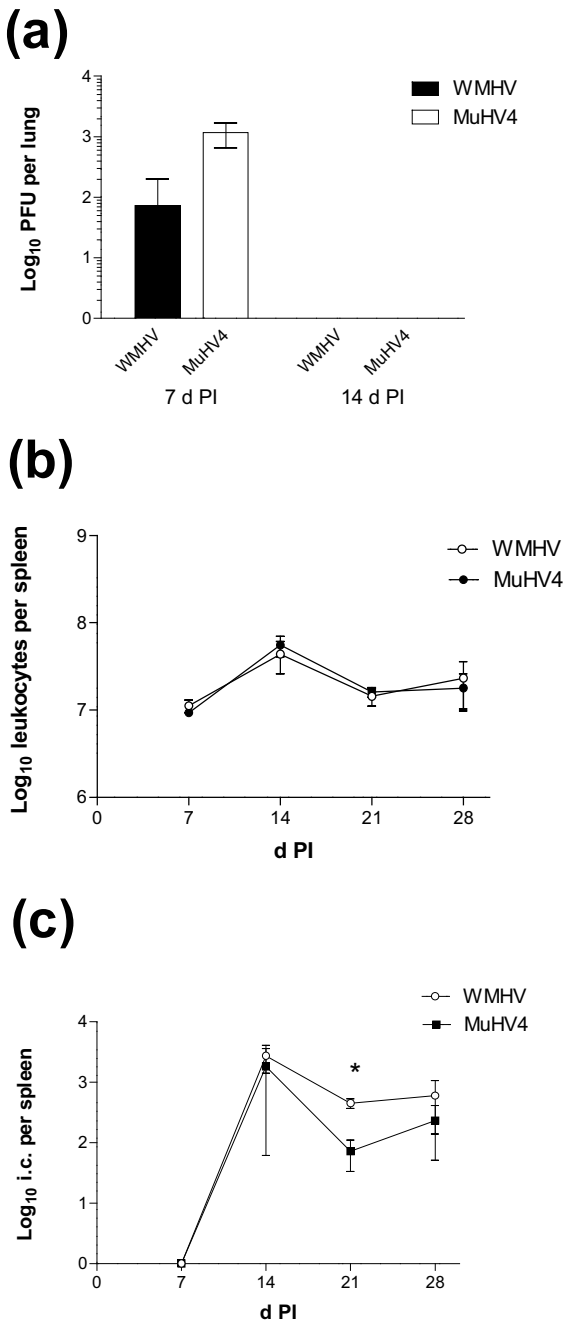
(a)
WMHV
MuHV4
Log10 PFU per lung
4
3
2
1
0
WMHV
MuHV4
WMHV
MuHV4
7 d PI
14 d PI
(b)
WMHV
MuHV4
Log10 leukocytes per spleen
9
8
7
6
0
7
14
21
28
d PI
(c)
WMHV
MuHV4
Log10 i.c. per spleen
4
3
2
1
0
*
0
7
14
21
28
d PI

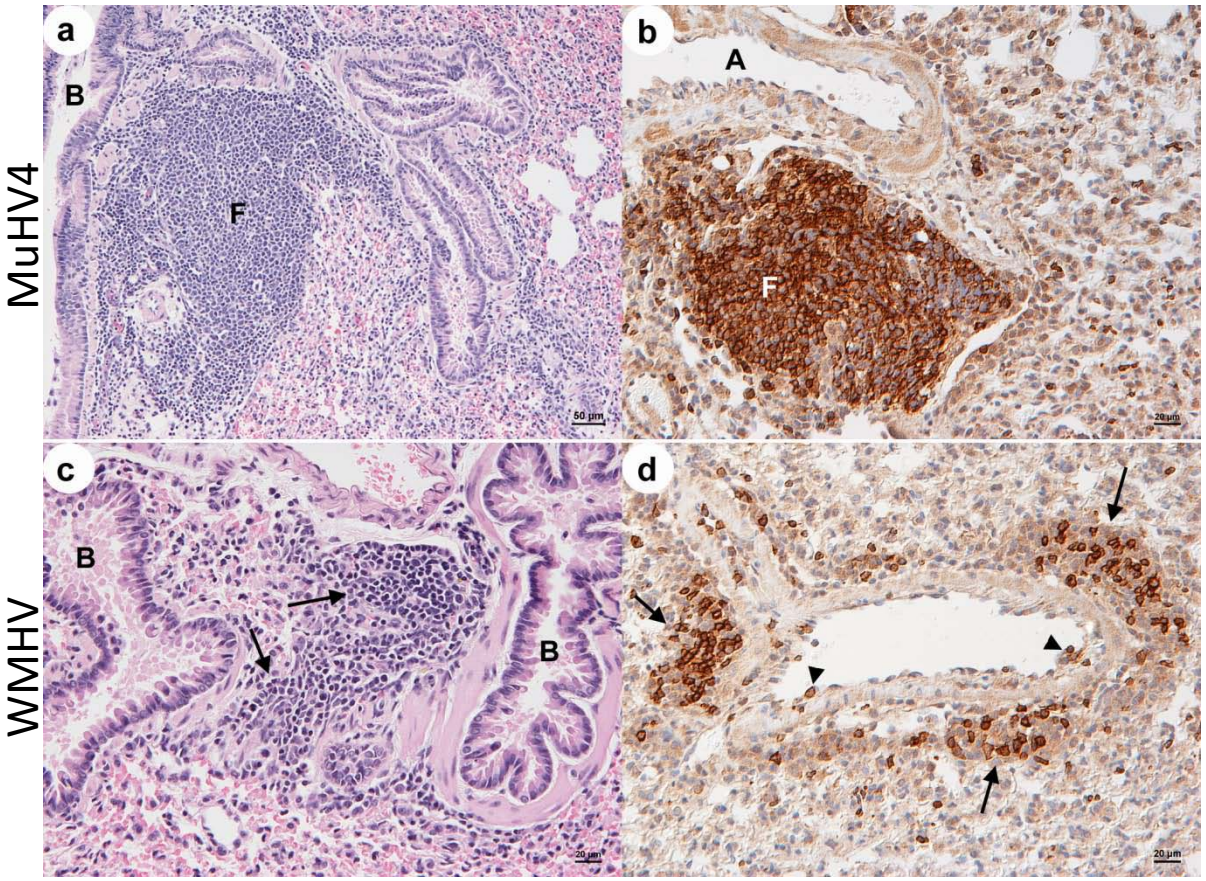
MuHV4
WMHV
a
B
F
50 µm
b
A
F
20 µm
c
B
B
20 µm
d
20 µm

Table S1. Information used to annotate the WMHV and MuHV4 genome sequences

	Protein name*	Family	Description	EC no.	Activity
M1	protein M1	M1	contains a signal peptide; secreted protein		unknown
M2	protein M2		interacts with Vav oncoprotein; involved in B cell proliferation and differentiation		immune regulation; latency
M3	chemokine-binding protein M3	M1	contains a signal peptide; secreted protein		immune regulation
M4	chemokine-binding protein M4	M1	contains a signal peptide; secreted protein		immune regulation
ORF4	complement control protein	CCP	type 1 envelope glycoprotein; contains four SCR domains		immune regulation
ORF6	single-stranded DNA-binding protein		contains a zinc-finger		DNA replication; possibly gene regulation
ORF7	DNA packaging terminase subunit 2				DNA encapsidation
ORF8	envelope glycoprotein B		type 1 membrane protein; possible membrane fusogen; binds cell surface heparan sulphate		cell entry; cell-to-cell spread
ORF9	DNA polymerase catalytic subunit			2.7.7.7	DNA replication
ORF10	protein G10	DURP			unknown
ORF11	virion protein G11	DURP			unknown
ORF12	E3 ubiquitin ligase MIR1	MIR	type 3 membrane protein; 2 transmembrane domains; contains a PHD finger; downregulates MHC-I		immune regulation
13M	protein 13M		hypothetical protein encoded by 5'-region of ORF12 transcript		unknown
ORF17.5	capsid scaffold protein		clipped near C terminus		capsid morphogenesis
ORF17	capsid maturation protease		serine protease (N-terminal region); minor scaffold protein (remainder of protein, clipped near C terminus)	3.4.21.97	capsid morphogenesis
ORF18	protein UL79		required for expression of late genes		gene regulation
ORF19	DNA packaging tegument protein UL25		located on capsid near vertices; possibly stabilizes the capsid and retains the genome		DNA encapsidation
ORF20	nuclear protein UL24				unknown
ORF21	thymidine kinase			2.7.1.21	nucleotide metabolism
ORF22	envelope glycoprotein H		type 1 membrane protein; possible membrane fusogen; complexed with envelope glycoprotein L		cell entry; cell-to-cell spread
ORF23	protein UL88				unknown
ORF24	virion protein UL87				unknown
ORF25	major capsid protein		6 copies form hexons, 5 copies form pentons		capsid morphogenesis
ORF26	capsid triplex subunit 2		complexed 2:1 with capsid triplex subunit 1 to connect capsid hexons and pentons		capsid morphogenesis
ORF27	envelope glycoprotein 48		type 2 membrane protein		cell-to-cell spread
ORF28	envelope glycoprotein 150		type 1 membrane protein		immune regulation
ORF29	DNA packaging terminase subunit 1		contains an ATPase domain		DNA encapsidation
ORF30	protein UL91				unknown
ORF31	protein UL92				unknown
ORF32	DNA packaging tegument protein UL17		capsid-associated		DNA encapsidation; capsid transport
ORF33	tegument protein UL16				possibly virion morphogenesis
ORF34	protein UL95				unknown
ORF35	tegument protein UL14				virion morphogenesis
ORF36	tegument serine/threonine protein kinase	PK		2.7.11.1	protein phosphorylation
ORF37	deoxyribonuclease				DNA processing
ORF38	myristylated tegument protein		envelope-associated		virion morphogenesis
ORF39	envelope glycoprotein M		type 3 membrane protein; 8 transmembrane domains; complexed with envelope glycoprotein N		virion morphogenesis; membrane fusion
ORF40	helicase-primase subunit				DNA replication
ORF42	tegument protein UL7				virion morphogenesis
ORF43	capsid portal protein		dodecamer located at one capsid vertex in place of a penton		DNA encapsidation

ORF44	helicase-primase helicase subunit				DNA replication
ORF45	tegument protein G45				unknown
ORF46	uracil-DNA glycosylase			3.2.2.3	DNA repair
ORF47	envelope glycoprotein L		complexed with envelope glycoprotein H		cell entry; cell-to-cell spread
ORF48	tegument protein G48				unknown
ORF49	protein G49		cooperates with protein Rta		gene regulation
ORF50	protein Rta				gene regulation; latency
ORF51	envelope glycoprotein 350		type 1 membrane protein		cell attachment
ORF52	virion protein G52				unknown
ORF53	envelope glycoprotein N		type 1 membrane protein; complexed with envelope glycoprotein M		virion morphogenesis; membrane fusion
ORF54	deoxyuridine triphosphatase	DURP		3.6.1.23	nucleotide metabolism
ORF55	tegument protein UL51				virion morphogenesis
ORF56	helicase-primase primase subunit				DNA replication
ORF57	multifunctional expression regulator	MER	RNA-binding protein; shuttles between nucleus and cytoplasm; inhibits pre-mRNA splicing; exports virus mRNA from nucleus; exerts most effects post-transcriptionally		gene regulation; RNA metabolism and transport
ORF58	envelope protein UL43		type 3 membrane protein; 11 transmembrane domains		possibly membrane fusion
ORF59	DNA polymerase processivity subunit		dsDNA-binding protein		DNA replication
ORF60	ribonucleotide reductase subunit 2			1.17.4.1	nucleotide metabolism
ORF61	ribonucleotide reductase subunit 1			1.17.4.1	nucleotide metabolism
ORF62	capsid triplex subunit 1		complexed 1:2 with capsid triplex subunit 2 to connect capsid hexons and pentons		capsid morphogenesis
ORF63	tegument protein UL37		complexed with large tegument protein		virion morphogenesis
ORF64	large tegument protein		complexed with tegument protein UL37; ubiquitin-specific protease (N-terminal region)		capsid transport
ORF65	small capsid protein		located externally on capsid hexons		capsid morphogenesis; possibly capsid transport
ORF66	protein UL49				unknown
ORF67	nuclear egress type 2 membrane protein		interacts with nuclear egress lamina protein		nuclear egress
ORF67A	DNA packaging protein UL33		interacts with DNA packaging terminase subunit 2		DNA encapsidation
ORF68	DNA packaging protein UL32				DNA encapsidation; possibly capsid transport
ORF69	nuclear egress lamina protein		interacts with nuclear egress type 2 membrane protein		nuclear egress
ORF72	cyclin				cell cycle regulation
M11	apoptosis regulator M11	Bcl-2			apoptosis
ORF73	nuclear antigen LANA		chromosome-tethering protein		latency
ORF74	membrane protein G74	GPCR	type 3 membrane protein; 7 transmembrane domains		intracellular signalling
ORF75C	tegument protein G75C	FGARAT			unknown
ORF75B	protein G75B	FGARAT			unknown
ORF75A	protein G75A	FGARAT			unknown

* Protein names are a provisional standard for all herpesviruses

Encoded by a core gene (i.e. inherited from an ancestor of alpha-, beta- and gammaherpesviruses)
Encoded by a betagamma gene (i.e. inherited from an ancestor of beta- and gammaherpesviruses)
Encoded by a gamma gene (i.e. inherited from an ancestor of gammaherpesviruses)
Encoded by a gene specific to a subset of gammaherpesviruses